Structural and Kinetic Investigations on the 15−21 and 42−45 Loops of Muscle Acylphosphatase: Evidence for Their Involvement in Enzyme Catalysis and Conformational Stabilization[†]

Niccolò Taddei,[‡] Fabrizio Chiti,[‡] Francesca Magherini,[‡] Massimo Stefani,*[,‡] Marjolein M. G. M. Thunnissen,[§] Pär Nordlund,[§] and Giampietro Ramponi[‡]

Department of Biochemical Sciences, University of Florence, Florence, Italy, and Department of Molecular Biology, University of Stockholm, Stockholm, Sweden

Received January 24, 1997; Revised Manuscript Received March 28, 1997[⊗]

ABSTRACT: The structural and catalytic importance of the 15−21 and 42−45 loop residues of the acylphosphatase muscular isoenzyme has been investigated by oligonucleotide-directed mutagenesis. Seven mutants involving conserved residues of the two loops have been prepared and characterized for structural, kinetic, and stability features by using different spectroscopic techniques and compared to the wild-type enzyme. The results are discussed in light of the crystal structure of the highly homologous common type acylphosphatase [Thunnissen et al. (1997) *Structure 5,* 69−79]. A differential role of the two loops has emerged: the 15−21 and the 42−45 loops appear mainly involved in active site formation and enzyme structural stabilization, respectively. These conclusions are supported by a strong impairment of the catalytic efficiency, in terms of enzymatic activity and substrate binding capability, for most of the 15−21 loop mutants. In particular, the Gly15Ala mutant is completely inactive and displays a native-like overall fold, indicating that the correct geometry of the 15−21 loop is an essential requisite for optimal enzymatic catalysis. Instead, the Gly45Ala mutant, though revealing unchanged catalytic properties, shows a considerably reduced conformational stability, as judged by circular dichroism and ^{1}H NMR spectroscopy. This finding confirms previous results relative to Thr42 and Thr46 residues [Taddei et al. (1996) *Biochemistry 35,* 7077−7083] underlining the structural importance of the 42−45 loop as a linker for the two $\beta\alpha\beta$ units constituting the overall enzyme structure.

Acylphosphatase is a cytosolic enzyme, generally formed by 98 amino acid residues, which catalyzes the hydrolysis of the carboxyl phosphate bond present in compounds of both synthetic and physiological significance such as 1,3-bisphosphoglycerate, carbamoyl phosphate, acetyl phosphate, and β-aspartyl phosphate (Stefani & Ramponi, 1995). Acylphosphatase is widely distributed among vertebrate species; very recently, two open-reading frames corresponding to the enzyme have been detected in *Drosophila* and *Escherichia coli* genomes, respectively (data bank AC AE000199 and L39752). Two acylphosphatase isoenzymes are currently known in vertebrate tissues, sharing over 55% sequence homology; their genes are thought to be originated by duplication and subsequent evolution of a common ancestor (Liguri et al., 1986; Fujita et al., 1987; Mizuno et al., 1990). The two isoenzymes are named muscular type and common (erythrocyte) type depending on the tissue where each isoenzyme is more abundant or it has been first isolated.

At present, no definitive data about the true physiological function of both acylphosphatase isoenzymes are available. Most experimental evidence suggests that, in vertebrates, they could be involved in the control of glycolysis (Ramponi, 1975) as well as in the regulation of intracellular ion homeostasis by their action on membrane ion pumps (Hokin et al., 1965; Stefani et al., 1981). In fact, it has been demonstrated that the acylphosphatase isoenzyme content is particularly high in tissues, such as skeletal muscle, brain, testis, heart, and retina, where glycolysis is very active. The enzyme activity sharply rises in chicken muscle after hatching, when glycolysis is fully activated (Ramponi et al., 1968; Ohba et al., 1989); in addition, yeast cells engineered with the acylphosphatase gene and overexpressing high amounts of enzyme are able to considerably enhance the speed of ethanol fermentation (Raugei et al., 1996). An uncoupling effect by acylphosphatase on transmembrane ion transport driven by membrane pumps has been demonstrated; acylphosphatase is able to interfere with ion transport by hydrolyzing the β-aspartyl phosphate intermediate formed during ATPase action (Nassi et al., 1991, 1993, 1994; Nediani et al., 1996). The possible alterations of intracellular levels of ions such as Na^+ and Ca^{2+} could be associated to the demonstrated effects of acylphosphatase on the intracellular phosphoinositide pattern (Berti et al., 1988), myoblast differentiation (Berti et al., 1992), and oocyte maturation (Dolfi et al., 1993a,b). At present, nothing is known about the functions performed by acylphosphatase in invertebrates and in prokaryotes.

Much more information is currently available on acylphosphatase structural and kinetic features. The muscular and erythrocyte isoenzymes were first sequenced in 1980 and in

[†] This work was supported by grants from EC (Contract ERB BIO4-CT96-0517) and from Italian CNR (target project Structural Biology).

* Address correspondence to the author at the Department of Biochemical Sciences, Viale Morgagni 50, 50134 Florence, Italy, Telephone: +39 55 413765. Fax: +39 55 4222725. Email: stefani@scibio.unifi.it.

[‡] University of Florence.

[§] University of Stockholm.

[⊗] Abstract published in *Advance ACS Abstracts,* May 15, 1997.

S0006-2960(97)00173-6 CCC: $14.00

1986, respectively (Cappugi et al., 1980; Liguri et al., 1986). At present, over 15 amino acid sequences of both isoenzymes from several vertebrate species are known, demonstrating they are highly conserved proteins (Pazzagli et al., 1993). This is confirmed by the *Drosophila* and *E. coli* open-reading frames corresponding to proteins with a significant sequence homology (30−40%) to vertebrate acylphosphatases. The possible presence of acylphosphatase homologues in lower organisms suggests differential physiological roles of this enzyme in lower and higher organisms. The solution structure of the muscular isoenzyme has been determined at low resolution by ^{1}H nuclear magnetic resonance (NMR)[1] spectroscopy (Pastore et al., 1992). The enzyme is a closely packed globular α/β protein showing a five-stranded antiparallel twisted β-sheet faced by two antiparallel α-helices running parallel to the sheet. The protein is composed of two intercalating $\beta\alpha\beta$ structural units arranged in a 4−1−3−2 β-strand topology. This fold has been found in other phosphate binding proteins showing no significant sequence homology to each other (Adman et al., 1973; Leijonmark & Liljas, 1987; Nagai et al., 1990; Coll et al., 1991; Erzberg et al., 1992; Eriksson & Salman, 1993).

The muscular isoenzyme catalytic mechanism was previously studied by a kinetic approach (Satchell et al., 1972); more recently, the residues involved in enzyme catalysis have been identified by an extensive oligonucleotide-directed mutagenesis investigation. Such a study allowed us to describe the role played by some conserved residues in the enzyme active site. In particular, Arg23 and Asn41 have emerged as the main phosphate binding site and the catalytic residue probably involved in the orientation and stabilization of the catalytic water molecule, respectively (Taddei et al., 1994a, 1996). However, no other catalytic residue(s) was (were) identified by this approach.

Recently, the crystal structure of the common type isoenzyme from bovine testis has been determined at 1.8 Å resolution (Thunnissen et al., 1997) (Figure 1). The three-dimensional structure is definitely comparable to that of the horse muscular isoenzyme previously determined by ^{1}H NMR spectroscopy. Local differences between the two structures have been described, mostly involving the loop regions, particularly the 15−21 loop. These differences were attributed to the presence of a sulfate ion and a chloride ion, both acylphosphatase competitive inhibitors, at the active site, which is formed in part by the backbone of the 15−21 loop. However, the presence of crystal contacts due to molecule packing in this region raised the question of a possible structural distortion of the active site. Acylphosphatase structural features arising from X-ray analysis confirmed the data obtained by the mutagenesis experiments indicated above and led to the proposal of a substrate-assisted catalytic mechanism (Thunnissen et al., 1997).

The structural data indicate the importance of the 15−21 loop for enzyme active site formation although the individual contribution of the single loop residues to catalysis has not yet been detailed; furthermore, previous results from a mutagenesis study underlined the importance of Thr42, belonging to loop 42−45, and of Thr46 for enzyme stability (Taddei et al., 1996). Taking into account that most of the residues in the 15−21 loop and some in the 42−45 loop are highly conserved in all acylphosphatases so far sequenced, including the *Drosophila* and *E. coli* open-reading frames, it seemed of remarkable interest to investigate in more detail the differential role performed by such loops in terms of catalytic importance and structural stability. We have therefore studied the kinetic, structural, and stability features of a number of muscle acylphosphatase mutants in the 15−21 and 42−45 loop regions by using different spectroscopic techniques. The results obtained are discussed in light of the common type acylphosphatase crystal structure.

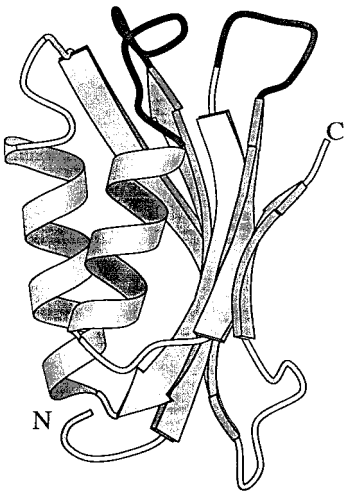

FIGURE 1: Schematic representation of acylphosphatase drawn using Molscript (Kraulis, 1991). The backbone of the 15−21 and 42−45 loop residues is in black. Atomic coordinates are from the common type isoenzyme crystal structure (Thunnissen et al., 1997).

MATERIALS AND METHODS

Materials. Benzoyl phosphate was synthesized according to Camici et al. (1976) and freshly dissolved before enzyme activity measurements. Isopropyl thiogalactoside (IPTG)[1] and restriction enzymes were from Promega. Sequenase was from USB; glutathione, thrombin, and glutathione affinity gel were purchased from Sigma. pGEX-2T was from Pharmacia. The pGEX-AP plasmid was prepared as previously described (Modesti et al., 1995). The plasmid is a derivative of the pGEX-2T plasmid in which a chemically synthesized gene coding for human muscle acylphosphatase was inserted (Modesti et al., 1993). Plasmid propagation and recombinant fusion protein expression were achieved in DH5α *E. coli* strain. Oligonucleotides harboring the desired mutated codons were from Pharmacia Biotech (Freiburg, Germany). The specific polyclonal anti-recombinant human muscle acylphosphatase antibodies used in the Western blotting were obtained from immunized rabbits as previously reported (Berti et al., 1982). Horseradish peroxidase-linked mouse anti-rabbit Ig was from BioRad. [α-^{32}P]ATP (800 Ci/mmol) and [^{32}P]P_i (8500 Ci/mmol) were from New England Nuclear. D_2O and acetic acid-d_4 were from Merck (Darmstadt, Germany). All other reagents were analytical grade or the best commercially available.

Site-Directed Mutagenesis. All acylphosphatase mutants (Gly15Ala, Val17Leu, Gln18Ala, Gly19Ala, Gly19Val,

[1] Abbreviations: Gly15Ala, glycine 15 to alanine mutant; Val17Leu, valine 17 to leucine mutant; Gln18Ala, glutamine 18 to alanine mutant; Gly19Ala and Gly19Val, glycine 19 to alanine and valine mutants, respectively; Val20Leu, valine 20 to leucine mutant; Gly45Ala, glycine 45 to alanine mutant; NMR, nuclear magnetic resonance; CD, circular dichroism; CED, cyanoethyldeoxy; IPTG, isopropyl thiogalactoside; SDS−PAGE, sodium dodecyl sulfate−polyacrylamide gel electrophoresis; USE, unique site elimination.

Val20Leu, Gly45Ala) were obtained by oligonucleotide-directed mutagenesis using a USE mutagenesis kit based on the unique site elimination (USE) method developed by Deng and Nickoloff (1992). Seven target primers harboring the desired mutated codons were previously synthesized by the CED-phosphoramidite method. Each primer carried one of the desired mutations [GGT or GGC (Gly) to GCC (Ala) or GTT (Val), GTG (Val) to CTC (Leu), and CAG (Gln) to GCC (Ala)]; the remaining primer sequence was complementary to the noncoding strand of the synthetic gene coding for human muscular acylphosphatase (Table 1). The method uses the target mutagenic primers and a selection primer to insert site-specific mutations into the plasmid; both mutations are then incorporated into the same strand by *in vitro* DNA synthesis. The selection primers eliminate the unique recognition sequence for the restriction enzyme *Apa*I in a nonessential region of the pGEX-2T plasmid. In our case, such mutagenized double-stranded DNAs were introduced by transformation in *E. coli* strain DH5α cells. The mutations were confirmed by DNA sequencing according to Sanger et al. (1977) and by amino acid analysis of the purified proteins.

Fusion Protein Expression and Recombinant Enzyme Purification. The expression of the recombinant mutated and wild-type acylphosphatase genes was achieved after inducing cell cultures with 0.2 mM IPTG under the conditions previously described (Taddei et al., 1996). The presence of the mutated proteins in cell lysates was assayed by SDS−PAGE analysis according to Laemmli (1970) and by Western blot analysis; the latter was performed by using anti-recombinant human muscle acylphosphatase antibodies and horseradish peroxidase-linked mouse anti-rabbit Ig. The fusion proteins were purified as previously reported (Modesti et al., 1995). Recombinant mutated and wild-type acylphosphatases were recovered from fusion proteins by thrombin cleavage and then purified from both glutathione *S*-transferase and unhydrolyzed fusion protein by gel filtration as previously indicated (Modesti et al., 1995; Taddei et al., 1996). The purified fusion proteins and the cleaved recombinant acylphosphatases were controlled by SDS−PAGE analysis.

Acylphosphatase Activity Measurements. Acylphosphatase activity was measured by a continuous optical test at 283 nm and pH 5.3 using benzoyl phosphate as a substrate as previously reported (Ramponi et al., 1966). The activity of the Gly15Ala mutant was determined by adding to the standard test mixture an amount of enzyme over 1000-fold higher as compared to that normally used.

Protein Determination and Amino Acid Analysis. Protein concentration was measured by either UV absorption, using $A^{1\%}_{1cm,280} = 14.2$ for all acylphosphatases, or amino acid analysis. Amino acid analyses were performed as previously described (Manao et al., 1983) using a Carlo Erba Model 3A29 amino acid analyzer equipped with a Hewlett-Packard HP3395 computing integrator. Values for threonine and serine were corrected taking into account degradation occurred during sample hydrolysis.

Equilibrium Dialysis. Equilibrium dialysis experiments were carried out at pH 5.3 and 4 °C. The enzyme concentration was 3−4 mg/mL, and 50 μL of both enzyme and dialysis solution was used in each compartment as previously reported (Taddei et al., 1994a). Dialysis solution contained differing concentrations of inorganic phosphate and [^{32}P]P_i at a specific radioactivity of 0.7 mCi/mmol. After equilibrium was attained, ^{32}P radioactivity was measured in each dialysis compartment, and the data were processed by Scatchard analysis.

^{1}H NMR Spectroscopy Measurements. ^{1}H NMR experiments were performed at 600 MHz in a temperature range of 30−70 °C, using a Bruker AMX600 NMR spectrometer. Wild-type and mutant acylphosphatase samples were prepared at a protein concentration of 5−6 mg/mL in 50 mM acetate-*d*/D_2O buffer, pH 3.8, and used for recording one-dimensional ^{1}H NMR spectra as previously reported (Taddei et al., 1995). 1,4-Dioxane was used as an internal shift reference at 3.74 ppm.

CD Experiments. Circular dichroism (CD) spectra were performed on a Jasco Model J-710 spectropolarimeter equipped with a thermostated cell holder and a NesLab Model RTE-110 water circulating bath. The instrument was calibrated with *d*-(+)-10-camphorsulfonic acid (Toumadje et al., 1992). Far-UV wild-type and mutated acylphosphatase spectra were recorded at 25 °C in 10 mM acetate buffer, pH 3.8, at a protein concentration of 0.10−0.25 mg/mL, using a 0.1 cm path-length quartz cell.

Thermal Unfolding. The heat denaturation transition for all samples was followed by ^{1}H NMR and CD. The melting temperature (t_m), defined as the temperature required to denature half of the molecules, was calculated for each enzyme by ^{1}H NMR by integrating well-resolved resonances from spectra acquired at increasing temperatures, as previously reported (Taddei et al., 1994b). Reversibility of thermal unfolding was determined by integration of the same resonances from spectra recorded upon cooling the denatured sample to 30 °C. Thermal denaturation experiments were also carried out by CD, at a protein concentration of 0.05−0.10 mg/mL in 10 mM acetate buffer, pH 3.8, using a 1 cm. path-length quartz cell heated (under continuous stirring) at a linear heating rate of 50 °C/h. The CD signal at increasing temperatures was recorded at 222 nm for each sample. Actual temperatures into the cell were recorded simultaneously to the CD signal, using a thermocouple. Reversibility of thermal unfolding was determined by measuring the recovery of the CD signal upon cooling to 25 °C protein samples. Thermal denaturation transition curves were analyzed according to the two-state model for the native (N) $\leftrightarrows$ D denatured (D) transition (Privalov, 1979; Taddei et al., 1994b). Thermodynamic parameters were calculated from CD data as previously described (Becktel & Schellman, 1987; De Filippis et al., 1995). Thermodynamic data were processed by the programme Kaleidagraph (Abelbeck, U.K.).

RESULTS

A number of recombinant muscle acylphosphatases carrying substitutions at Gly15, Val17, Gln18, Gly19, Val20, and Gly45 positions (strictly conserved in all acylphosphatases sequenced so far) have been obtained by overexpressing in *E. coli* strain DH5α cells the synthetic gene for the human muscle enzyme properly mutated at each of the above-mentioned positions. Oligonucleotide-directed mutagenesis was performed by using the synthetic oligonucleotides shown in Table 1 under the conditions reported under Materials and Methods. Wild-type and mutated recombinant enzymes were purified from cell lysates as fusion proteins with glutathione *S*-transferase and subsequently cleaved by

Table 1: Sequences of the Oligonucleotides Used for the Production of the Mutated Enzymes[a]

enzyme	oligonucleotide sequence
wild-type (15−21...45)[b]	5′ GGTCGCGTGCAGGGCGTGTGC...GGT 3′
Gly15Ala	5′ CGAGGTCTTT**GCC**CGCGTGCAGG 3′
Val17Leu	5′ CTTTGGTCGC**CTC**CAGGGCGT 3′
Gln18Ala	5′ TGGTCGCGTG**GCC**GGCGTGTGC 3′
Gly19Ala	5′ CGCGTGCAG**GCC**GTGTGCTTTC 3′
Gly19Val	5′ CGCGTGCAG**GTT**GTGTGCTTTC 3′
Val20Leu	5′ GTGCAGGGC**CTC**TGCTTTCGTA 3′
Gly45Ala	5′ CACCAGCAAA**GCC**ACCGTGACCG 3′

[a] The mutated codons are in boldface type. [b] The wild-type nucleotide sequence refers to the synthetic gene coding for human muscle acylphosphatase (Modesti et al., 1993).

Table 2: Main Kinetic Parameters Calculated from Activity Measurements and Equilibrium Dialysis Experiments[a]

enzyme	specific activity (IU/mg)	pH optimum	K_m (mM)	K_i (mM)	k_{cat}/K_m (mM^{-1} s^{-1})
wild-type	6500	4.8−5.8	0.34 ± 0.04	0.75 ± 0.13	3600
Gly15Ala	2	nd	nd	>10.0[b]	nd
Val17Leu	70	4.7−5.8	0.95 ± 0.08	5.08 ± 0.38	14
Gln18Ala	390	4.9−5.8	0.71 ± 0.03	1.96 ± 0.28	100
Gly19Ala	5300	4.7−5.7	0.45 ± 0.04	1.80 ± 0.39	2200
Gly19Val	3800	4.7−5.7	1.74 ± 0.11	10.5 ± 1.6	410
Val20Leu	440	4.8−5.8	1.77 ± 0.13	2.56 ± 0.48	47
Gly45Ala	5000	4.8−5.8	0.34 ± 0.06	1.12 ± 0.20	2800

[a] One IU is defined as the enzyme activity that liberates 1 μmol/min of benzoate, at pH 5.3 and 25 °C. The pH optimum was calculated at 25 °C in 0.1 M acetate buffer, pH 3.7−6.5, and in 50 mM 3,3-dimethylglutarate buffer, pH 6.0−7.5. The other parameters were determined in 0.1 M acetate buffer, pH 5.3. K_m and K_i were calculated kinetically using benzoyl phosphate and inorganic phosphate as substrate and competitive inhibitor, respectively. nd is not determined. [b] Value determined as K_d from equilibrium dialysis experiment in 0.1 M acetate buffer, pH 5.3.

thrombin with overall purification yields averaging 2−3 mg of protein/L of culture. Hydrophobic and hydrophilic residues were substituted in order to minimally increase the steric hindrance of their side chains and to eliminate their hydrogen bonding capability, respectively. Therefore, Gly15, Gln18, and Gly45 were replaced by alanine; Val17 and Val20 were replaced by leucine; and Gly19 was replaced by either alanine or valine. The effectiveness of the mutational insertion was checked, for each gene, by DNA sequencing according to Sanger's method and further confirmed by amino acid analysis of the purified enzymes (data not shown). The homogeneity of the cleaved recombinant acylphosphatases was assessed by SDS−PAGE analysis (data not shown). The kinetic, structural, and stability features of the purified wild-type and mutant enzymes were investigated.

Table 2 summarizes the main kinetic parameters as determined for all the studied enzymes under the conditions reported under Materials and Methods. As predictable, all mutated enzymes showed their highest activity in a pH range comparable to that of the wild-type enzyme, since none of the mutations involved charged residues. For this reason, all kinetic parameters were determined at pH 5.3. Most mutations, namely, Val17Leu, Gln18Ala, and Val20Leu, determined a sharp reduction in enzymatic activity (1−6% of the wild-type specific activity). In the same mutants, a significant increase, though to a different extent, of the values of the apparent K_m for benzoyl phosphate, an acylphosphatase substrate, and K_i for inorganic phosphate, an acylphosphatase competitive inhibitor, was also observed. Such kinetic properties suggested that mutations at positions 17, 18, and 20 are responsible for a catalytic impairment partly attributable to a decrease of the substrate binding capability. The mutations at positions 19 and 45 were not responsible for a significant loss of enzymatic activity, and the mutated enzymes at these positions elicited 60−80% of the wild-type enzyme activity. The binding parameters for these mutants were similar to those of the wild-type enzyme, with the exception of the Gly19Val mutant that showed a significant increase of the K_m and K_i values. Interestingly, the mutant Gly15Ala did not show an appreciable activity under the standard assay conditions. In this case, the addition of a thousandfold higher amount of mutated enzyme to the assay reaction mixture enabled us to measure a residual 0.03% of the activity shown by the wild-type enzyme. Since the Gly15Ala mutant was almost completely devoid of enzymatic activity, it was not possible to precisely assess its binding properties through kinetic methods. It therefore seemed reasonable to attempt a different approach by performing an equilibrium dialysis experiment. This kind of experiment is based on the differential distribution of a ligand between two dialysis compartments containing the enzyme and the buffer, respectively, as a consequence of the affinity of the ligand for the enzyme (Reinard & Jacobsen, 1989). For our purpose, radioactive inorganic phosphate, a well-known acylphosphatase competitive inhibitor, was used. Figure 2 shows the Scatchard analysis of the data obtained from the equilibrium dialysis experiment. The apparent K_d value for the Gly15Ala mutant, hardly calculated from the slope of the $[E{\cdot}P_i]/[P_i]$ vs $[E{\cdot}P_i]$ curve, was about 9.8 mM. The difference in radioactivity between the two dialysis compartments was really low, at the resolution limit of the experiment; therefore, it would be more correct to say that the K_d value for inorganic phosphate relative to the Gly15Ala mutant is higher than 10 mM. The enzyme concentration used in each experiment was confirmed by the intercepts on the *x* axis. It is clear that the substrate/competitive inhibitor binding capability of the Gly15Ala mutant is strongly reduced as compared to that of the wild-type enzyme, but not completely abolished.

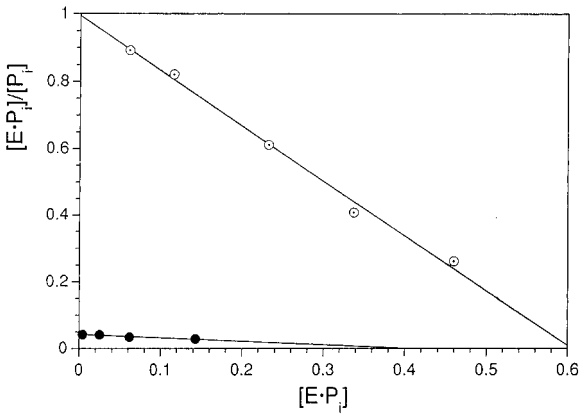

FIGURE 2: Scatchard analysis of the data obtained from the equilibrium dialysis experiment in the presence of varying $[^{32}P]P_i$, in 50 mM acetate buffer, pH 5.3 and 4 °C. (⊙) Wild-type acylphosphatase; (●) Gly15Ala mutant.

The effects of residue replacement on the kinetic properties of the mutated enzymes, particularly the Gly15Ala mutant, might be attributed to a major conformational change of the

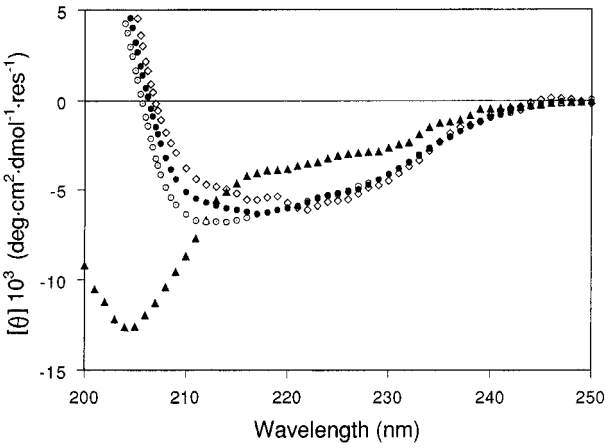

FIGURE 3: Far UV CD spectra of muscle acylphosphatases recorded in 10 mM acetate buffer, pH 3.8, 25 °C: (⊙) wild-type enzyme; (◇) Gly15Ala mutant; (●) Gly45Ala mutant. Thermally denatured (80 °C) wild-type enzyme is represented as (▲).

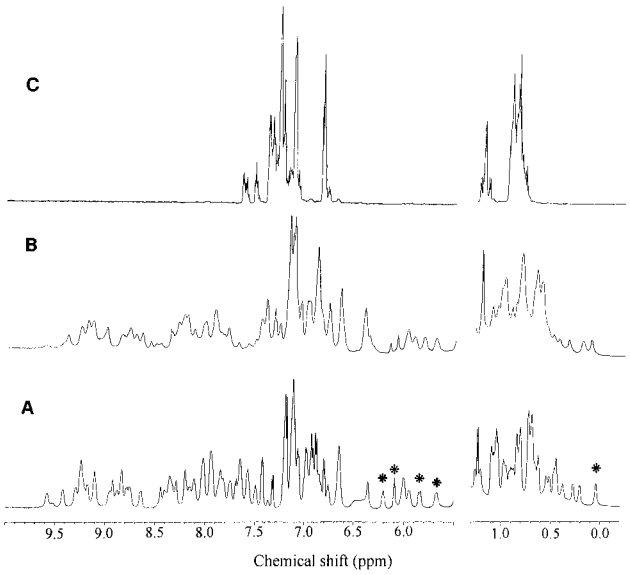

FIGURE 4: Aromatic and aliphatic regions of the 600 MHz spectra of muscle acylphosphatases, acquired in 50 mM acetate, pH 3.8, 30 °C. (A) Wild-type enzyme; (B) Gly15Ala mutant. Thermally denatured (70 °C) wild-type enzyme is represented in (C). Stars indicate the native resonances followed during thermal denaturation.

mutants. For this reason, the structural features of the recombinant wild-type and mutated enzymes were studied by CD and monodimensional ^{1}H NMR experiments. Figure 3 shows the far-UV CD spectra of the wild-type enzyme (both in its native and in its heat-denatured conformations) and of the Gly15Ala and Gly45Ala mutants. It is evident that all the enzymes in their native form display similar spectra, mainly in the region above 220 nm, indicating a substantially conserved secondary structure content. However, the CD signals of the two mutants, particularly the Gly15Ala mutant, in the 210 nm region appear slightly decreased as compared to that of the wild-type native enzyme. It is generally accepted that the negative CD band in the 210−220 nm region is characteristic of antiparallel β-sheets in proteins, although the position and relative and absolute intensities of this band may vary (Curtis Johnson, 1988, and references cited therein). A CD signal decrease similar to that shown by the Gly15Ala mutant is also observed in the other mutants of the acylphosphatase 15−21 loop (data not shown); this decrease could be attributed to a minor structural rearrangement of the β-sheet due to the replacement of the loop residues. The aliphatic and aromatic resonance regions of the 600 MHz ^{1}H NMR monodimensional spectra of the wild-type (native and thermally denatured) and Gly15Ala recombinant acylphosphatases are shown in Figure 4. The spectra of both the native wild-type enzyme and the mutant are characterized by a remarkable chemical shift dispersion and by the persistence of the backbone amide proton resonances. Such spectral features are indicative of a well-constrained tertiary structure typical of a fully folded protein (Wüthrich, 1986). A careful comparison of the two spectra indicates that there are some minor differences in the chemical shift of a number of resonances attributable to local changes in the three-dimensional structure. However, the ^{1}H NMR spectrum of the Gly15Ala mutant suggests that this mutant possesses a native-like global fold. The ^{1}H NMR spectra of all other mutants are definitely similar to each other and to the spectrum of the wild-type native enzyme (data not shown), indicating that none of the residue replacements performed in this study are responsible for major conformational changes.

In spite of the absence of relevant changes in the overall fold of the mutated enzymes, it seemed interesting to investigate the effect of residue substitutions on the stability of the different mutants. Thermal denaturation experiments were carried out at pH 3.8 by ^{1}H NMR and CD spectroscopy. Figure 4 shows the well-resolved resonances whose areas have been used as probes to evaluate the populations of folded and unfolded enzyme molecules and, therefore, to calculate the unfolding equilibrium constants at different temperatures. Such resonances refer to aromatic, backbone amide, and aliphatic protons distributed in different regions of the enzyme molecule, as previously reported (Taddei et al., 1994b). The t_m values calculated by ^{1}H NMR spectroscopy denaturation experiments are reported in Table 3. A more detailed study on mutant thermal stability was performed by CD spectroscopy. Figure 5A shows the thermal denaturation curves relative to the wild-type, Gly15Ala, Gly19Val, and Gly45Ala mutants following the CD signal at 222 nm. The three mutants show a two-state denaturation transition and, similarly to the wild-type enzyme, maintain a residual CD signal in the thermally denatured state. A comparable behavior was also found for all other mutants (data not shown). The comparative analysis of the thermodynamic data reported in Table 3 indicates that all mutants,

Table 3: Thermodynamic Parameters Relative to the Thermal Transition Curves from CD Data[a]

enzyme	t_m (°C)	ΔH_m (kJ mol^{-1})	ΔS_m (J deg^{-1}mol)	$\Delta\Delta G_{D,m}$ (kJ mol^{-1})
wild-type	60.6 ± 1.1 (58.0)[b]	266 ± 13	798 ± 25	−
Gly15Ala	53.0 ± 0.8 (53.5)	259 ± 9	794 ± 14	−6.0
Val17Leu	57.3 ± 0.6 (55.3)	225 ± 6	684 ± 10	−2.3
Gln18Ala	54.7 ± 0.7 (55.8)	201 ± 6	614 ± 12	−3.6
Gly19Val	51.3 ± 0.5 (53.7)	171 ± 8	528 ± 18	−4.9
Val20Leu	55.1 ± 0.9 (53.3)	242 ± 9	738 ± 15	−4.1
Gly45Ala	51.0 ± 0.6 (49.8)	246 ± 7	761 ± 13	−7.3

[a] Thermodynamic parameters were calculated as reported under Materials and Methods. t_m is the temperature required to unfold 50% of the enzyme molecules. ΔH_m and ΔS_m are the values of ΔH_D and ΔS_D calculated at the t_m. $\Delta\Delta G_{D,m}$ is the difference between the free energy of unfolding of each mutant and that of the wild-type enzyme at the t_m of the wild-type enzyme (Becktel & Schellman, 1987). [b] In parentheses, the t_m value calculated by ^{1}H NMR.

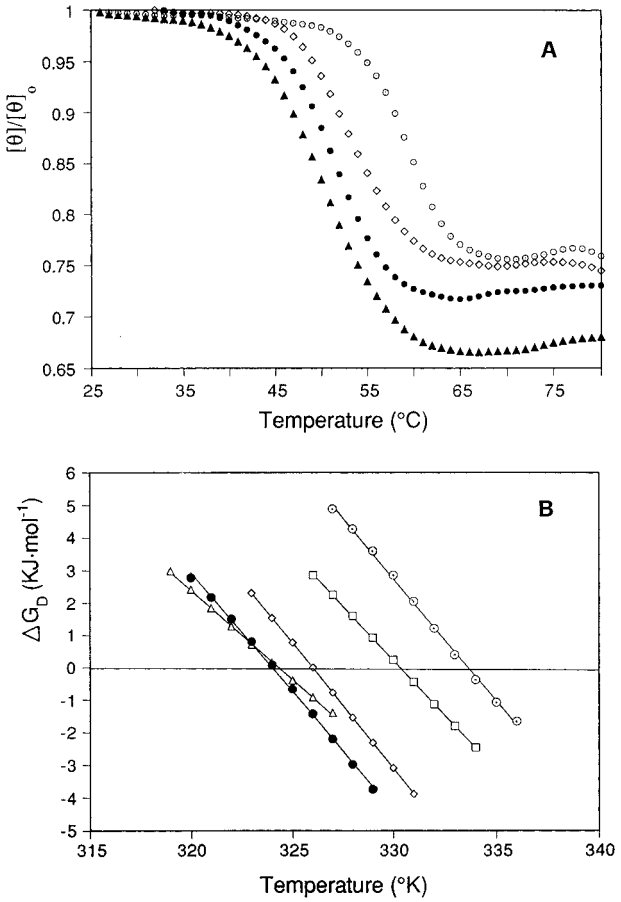

FIGURE 5: (A) Thermal denaturation of muscle acylphosphatases followed by recording the CD signal at 222 nm as a function of the sample temperature, in 10 mM acetate buffer, pH 3.8. Protein concentration was comparable for all samples (0.05−0.10 mg/mL). (⊙) Wild-type enzyme; (◇) Gly15Ala mutant; (▲) Gly19Val Mutant; (●) Gly45Ala mutant. (B) Temperature dependence of the free-energy change, ΔG_D, monitored during thermal denaturation of acylphosphatases: (⊙) Wild-type enzyme; (◇) Gly15Ala mutant; (□) Val17Leu mutant; (▲) Gly19Val mutant; (●) Gly45Ala mutant.

though to a different extent, feature t_m values lower than that of the wild-type enzyme (Figure 5B); this is accompanied by a decrease of conformational stability, as suggested by the $\Delta\Delta G_{D,m}$ values. The t_m values calculated from CD data do not significantly differ from those calculated from ^{1}H NMR data. $\Delta\Delta G_{D,m}$ values calculated from CD data for each mutant, ranging between −2.3 and −7.3 kJ/mol, become very indicative of a decrease of conformational stability when compared to the $\Delta G(H_2O)$ value at 37 °C (≈17 kJ/mol) previously reported for the wild-type enzyme (Taddei et al., 1994b, 1996). In particular, the Gly45Ala mutant is less stable than any of the 15−21 loop mutants, although its kinetic parameters are strictly similar to those of the wild-type enzyme. Among the 15−21 loop mutants, the Gly15Ala and Gly19Val mutants show the most different thermodynamic parameters as compared to the wild-type enzyme. Furthermore, the Gly19Val mutant reveals the lowest ΔH_m and ΔS_m values, suggesting that this mutant is less compact and more flexible as compared to the wild-type enzyme, as could be predicted by the replacement of the glycine by a bulky valine. The thermal unfolding reversibility was demonstrated for all enzymes by acquiring ^{1}H NMR spectra and measuring the CD signal at 222 nm after cooling the thermally denatured sample. In both cases, the mutants recovered over 85% of the native features (data not shown), similarly to the wild-type enzyme (Taddei et al., 1994b).

DISCUSSION

The NMR solution structure of muscle acylphosphatase indicates that both 15−21 and 42−45 loops are highly mobile parts of the protein (Saudek et al., 1989; Pastore et al, 1992); the crystal structure of the common type isoenzyme reveals that the two loops, particularly the 15−21 loop, have a distinct conformation possibly arising from the presence of a sulfate and a chloride ion at the active center. Since the two isoenzymes share 55% sequence homology, the effects of the mutations will be discussed on the basis of the conformation observed in the common type acylphosphatase structure (Figure 1). Figure 6 shows a stereo diagram of the 15−21 and 42−45 loops from the common type crystal structure, where nonconserved residues 16, 21, 43, and 44 have been replaced by those found in muscle acylphosphatase; the loops were consequently remodeled though their original structural features were fully conserved. Table 4 reports the hydrogen bonds and the torsion angles relative to the 15−21 and 42−45 residues. It can be observed that some residues, namely, Gly15, Gly19, Phe21, and Gly45, have special ϕ/ψ combinations. Gly15 is probably of great

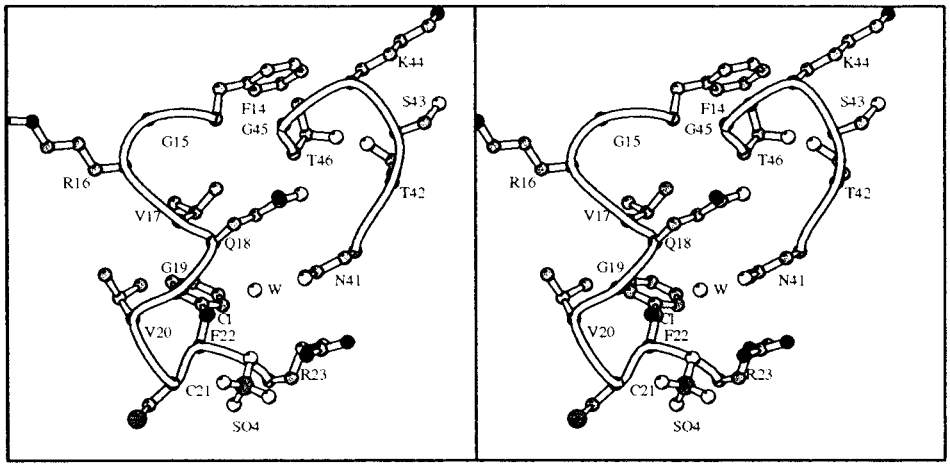

FIGURE 6: Stereo image of the 15−21 and 42−45 loops taken from the common type acylphosphatase crystal structure (Thunnissen et al., 1997). Residues 16, 21, 43, and 44 have been replaced by the residues present in the muscle isoenzyme. Such a replacement has been followed by structure modelling. A sulfate ion together with a chloride ion and the catalytic water molecule are also represented in the picture.

Table 4: Hydrogen Bonds and Torsion Angles Relative to the 15−21 and 42−45 Loop Residues[a]

hydrogen bonds (distances in Å)	residue	torsion angle (deg)		
		ϕ	ψ	ω
Gly15 O−N Val17 (3.27)	Gly15	136.3	−142.3	177.2
Lys16 N−O His74 (2.82)	Lys16	−98.7	89.4	−175.8
Lys16 O−N His74 (3.01)	Val17	−125.4	7.0	176.6
Phe21 O−N Tyr25 (3.11)	Gln18	−119.8	153.6	179.7
Gln18 Oϵ1−N Thr46 (3.36)	Gly19	66.2	22.0	−179.1
Gln18 Oϵ1−N Thr42 (3.77)	Val20	−131.7	23.7	−179.5
Gly45 N−O Thr42 (3.58)	Phe21	64.1	27.5	−179.0
Thr42 N−O Thr46 (2.94)				
Val17 O−H_2O (2.72)				
Asn41 Oδ1−H_2O (2.58)	Thr42	−103.3	172.3	179.3
Gly19 N−Cl^- (3.06)	Asp43	−79.5	0.7	180.0
Val20 N−Cl^- (2.95)	Gln44	−106.0	16.1	178.1
Phe21 N−Cl^- (3.12)	Gly45	81.4	13.6	−178.9
Phe21 N−SO_4^{2-} (3.50)	Thr46	−115.3	179.7	−179.6

[a] Data were obtained from the common type acylphosphatase crystal structure (Thunnissen et al., 1997) using the program XmMol 3.01.

importance since it is positioned at the end of the first β-strand: it is part of a tight β-turn that breaks the β-strand off and starts the loop. Another residue at this site, for example, the replacing alanine used in our study, would not be able to have the same ϕ/ψ combination, and therefore the loop conformation would have to be strongly different. This interpretation of structural data, in spite of the fact that Gly15 is 10 Å away (on average) from the active site, is consistent with the complete loss of catalytic activity of the Gly15Ala mutant. The different conformation of the loop and a subsequent minor rearrangement of the β-sheet (as indicated by CD data) resulting from mutation at position 15 are responsible for both an impaired binding and, most important, a wrong positioning of the substrate together with a significant destabilization of the overall enzyme structure. Further structural investigations are needed to confirm this behavior; for this purpose, we are currently trying to get high quality crystals of the Gly15Ala mutant.

The position of the sulfate ion at the active center, as is shown in Figure 6 and indicated by hydrogen bonding in Table 4, suggests that the loop residues mainly involved in binding and orienting the substrate are those located after position 19, and that glycine 19 has a critical role in stabilizing the conformation of the final part of the loop. Surprisingly, the replacement of Gly19 with alanine or valine did not determine the expected alterations of the catalytic properties. This result confirms that the sulfate, in the active site pocket, is somewhat pushed away by the chloride ion and, consequently, that the true position of the sulfate ion in the active pocket should probably be deeper (Thunnissen et al., 1997). The significant destabilizing effect due to Gly19 replacement can be explained considering that glycine has a higher tolerance for ϕ/ψ combination in the left-handed helix conformation than valine (Table 4); the absence of conformational stress will yield a more stable protein (Stites et al., 1994).

Mutation of Val17 to leucine also has an effect on the catalytic activity of the enzyme (1% as compared to the wild-type activity). In the common type acylphosphatase structure, this residue fits very snugly inside a hydrophobic pocket formed by residues Ile13, Phe22, Val47, and Ile75. The replacement of valine with the more bulky leucine probably has an effect on the residues lining the pocket; alternatively, the residue assumes a slightly different conformation responsible for a significant impairment of both catalysis and substrate binding. Similarly to Val17, Val20 replacement effects on catalysis can be explained in light of the common type crystal structure. Val20 occupies a more shallow pocket on the surface of the protein where it makes contacts with the Cβ of Ser73, the Cα of Val17, and the Cβ and Cγ of Lys16. Although this pocket is much shallower than that occupied by Val17, a larger residue, such as leucine, would need more space, allowing partial disruption of the loop and consequent catalytic impairment. The mutation of Gln18 to alanine is also responsible for the considerable alteration of the catalytic properties. In the common type acylphosphatase structure, this replacement would eliminate the hydrogen bonds between the glutamine side chain and the Thr42 and Thr46 main chain atoms (Table 4); in addition, the Gln18 side chain is remarkably close to the catalytic Asn41 (4−4.2 Å on average, Figure 6), though there are no hydrogen bonds between these residues. Both kinetic and structural data indicate that Gln18 plays an essential role in the stabilization of the loop conformation required for catalysis to occur. The conformational stability of the Val17Leu, Gln18Ala, and Val20Leu mutants, expressed in terms of $\Delta\Delta G_{D,m}$, is slightly reduced as compared to that of the wild-type enzyme, as can be expected for the replacement of residues playing nonessential roles in structural stabilization (Matouschek et al., 1994).

The replacement of Gly45 with alanine does not significantly change acylphosphatase kinetic parameters. However, among all mutants investigated, the Gly45Ala mutant shows the lowest conformational stability as compared to the wild-type enzyme. Such a result is consistent with previous data obtained for Thr42 and Thr46 mutants, whose conformational stability was similarly reduced (Taddei et al., 1996). The experimental results clearly show that the 42−45 loop distortion caused by Thr42, Gly45, and Thr46 substitutions does not influence enzyme catalysis (Table 2) (Taddei et al., 1996). In spite of the spatial proximity of the 42−45 loop to the active site residue Asn41 and to the catalytic 15−21 loop, the replacement of the conserved residues belonging to this loop is responsible for minor, kinetic consequences but determines serious effects on the enzyme stability, as is demonstrated by the destabilizing energy expressed by $\Delta\Delta G_{D,m}$ (Matouschek et al., 1994). In the common type acylphosphatase crystal structure, the 42−45 loop forms a tight type I β-turn connecting strands 2 and 3 of the β-sheet, and its conformation is stabilized by a number of hydrogen bonds (Table 4). Furthermore, Gly45 shows an unusual ϕ/ψ combination typical of the left-handed helix. The acylphosphatase structure can be considered as composed of two $\beta\alpha\beta$ subdomains intercalated into each other (Pastore et al., 1992). Interestingly, the 42−45 loop connects such two subdomains, and its modification could be responsible for subdomain misalignment followed by a decrease of the overall enzyme conformational stability.

The results reported in this paper indicate that the 42−45 loop indeed plays a critical role in the stabilization of the acylphosphatase overall structure; the same results underline that the 15−21 loop is part of the acylphosphatase active site and that its integrity is a fundamental requisite for an optimal enzyme catalytic performance. In particular, the essential importance of glycine 15 in the maintenance of the correct 15−21 loop conformation and the partial contribution

of the other highly conserved loop residues in such a role are highlighted, whereas glycine 19 plays a secondary role in determining the correct loop conformation. Further structural investigation of such mutants through X-ray crystallography (currently in progress) will provide new insights into acylphosphatase structure−function relationships.

ACKNOWLEDGMENT

CD experiments and ^{1}H NMR measurements were carried out at CRIBI Biotechnology Centre, University of Padova (Italy), and at the Laboratorio di Risonanze Magnetiche of the University of Florence (Italy), respectively. We thank Dr. V. De Filippis for assistance in CD experiments, Dr. L. Pazzagli for amino acid analysis, and M. Lucci for technical support in NMR experiments. The program XmMol 3.01 is a generous gift from Dr. P. Tuffery (France).

REFERENCES

Adman, F. T., Sicker, L. C., & Jensen, L. H. (1972) *J. Biol. Chem. 248*, 3987−3996.

Becktel, W. J., & Schellman, J. A. (1987) *Biopolymers 26*, 1859−1877.

Berti, A., Liguri, G., Stefani, M., Nassi, P., & Ramponi, G. (1982) *Physiol. Chem. Phys. 14*, 307−311.

Berti, A., Stefani, M., Degl'Innocenti, D., Ruggiero, M., Chiarugi, V., & Ramponi, G. (1988) *FEBS Lett. 235*, 229−232.

Berti, A., Degl'Innocenti, D., Stefani, M., & Ramponi, G. (1992) *Arch. Biochem. Biophys. 294*, 261−264.

Camici, G., Manao, G., Cappugi, G., & Ramponi, G. (1976) *Experientia 22*, 705.

Cappugi, G., Manao, G., Camici, G., & Ramponi, G. (1980) *J. Biol. Chem. 255*, 6868−6874.

Coll, M., Guasch, A., Aviles, F. X., & Huber, R. (1991) *EMBO J. 10*, 1−9.

Curtis Johnson, W., Jr. (1988) *Annu. Rev. Biophys. Biophys. Chem. 17*, 145−166.

De Filippis, V., Vindigni, A., Altichieri, A., & Fontana, A. (1995) *Biochemistry 34*, 9552−9564.

Deng, W. P., & Nickoloff, J. A. (1992) *Anal. Biochem. 200*, 81.

Dolfi, F., Carnero, A., Ramponi, G., & Lacal, J. C. (1993) *FEBS Lett. 326*, 167−170.

Dolfi, F., Carnero, A., Cuadrado, A., Ramponi, G., & Lacal, J. C. (1993) *FEBS Lett. 327*, 265−270.

Eriksson, P. O., & Salman, L. (1993) *J. Biomol. NMR 3*, 613−626.

Fujita, H., Mizuno, Y., & Shiokawa, H. (1987) *J. Biochem. (Tokyo) 102*, 1405−1414.

Hokin, I. E., Sastry, P. S., Galsworthy, P. R., & Yoda, A. (1965) *Proc. Natl. Acad. Sci. U.S.A. 54*, 177−184.

Kraulis, P. (1991) *J. Appl. Crystallogr. 24*, 946−950.

Laemmli, U. K. (1970) *Nature 227*, 680−685.

Leijonmark, M., & Liljas, A. (1987) *J. Mol. Biol. 195*, 555−580.

Liguri, G., Camici, G., Manao, G., Cappugi, G., Nassi, P., Modesti, A., & Ramponi, G. (1986) *Biochemistry 25*, 8089−8094.

Manao, G., Camici, G., Stefani, M., Berti, A., Cappugi, G., Liguri, G., Nassi, P., & Ramponi, G. (1983) *Arch. Biochem. Biophys. 226*, 414−424.

Matouschek, A., Serrano, L., & Fersht, A. R. (1994) *Analysis of protein folding by protein engineering* in *Mechanism of protein folding* (Pain, R. H., Ed.) pp 137−159, IRL press at Oxford University Press, Oxford, U.K.

Mizuno, Y., Ohba, Y., Fujita, H., Kanesaka, Y., Tamura, T., & Shiokawa, H. (1990) *Arch. Biochem. Biophys. 278*, 437−443.

Modesti, A., Raugei, G., Taddei, N., Marzocchini, R., Vecchi, M., Camici, G., Manao, G., & Ramponi, G. (1993) *Biochim. Biophys. Acta 1216*, 369−374.

Modesti, A., Taddei, N., Bucciantini, M., Stefani, M., Colombini, B., Raugei, G., & Ramponi, G. (1995) *Protein Expression Purif. 6*, 799−805.

Nagai, K., Oubridge, C., Jessen, T. H., & Evans, P. R. (1990) *Nature 348*, 515−520.

Nassi, P., Nediani, C., Liguri, G., Taddei, N., & Ramponi, G. (1991) *J. Biol. Chem. 26*6, 10867−10871.

Nassi, P., Marchetti, E., Nediani, C., Liguri, G., & Ramponi, G. (1993) *Biochim. Biophys. Acta 1147*, 19−26.

Nassi, P., Nediani, C., Fiorillo, C., Marchetti, E., Liguri, G., & Ramponi, G. (1994) *FEBS Lett. 337*, 109−113.

Nediani, C., Fiorillo, C., Marchetti, E., Pacini, A., Liguri, G., & Nassi, P. (1996) *J. Biol. Chem. 271*, 19066−19073.

Ohba, Y., Mizuno, Y., & Shiokawa, H. (1989) *J. Biochem. (Tokyo) 105*, 173−177.

Pastore, A., Saudek, V., Ramponi, G., & Williams, R. J. P. (1992) *J. Mol. Biol. 224*, 427−440.

Pazzagli, L., Cappugi, G., Camici, G., Manao, G., & Ramponi, G. (1993) *J. Protein Chem. 12*, 593−601.

Privalov, P. L. (1979) *Adv. Protein Chem. 33*, 167−241.

Ramponi, G. (1975) *Adv. Enzymol. 42*, 409−426.

Ramponi, G., Treves, C., & Guerritore, A. (1966) *Experientia 22*, 1019−1023.

Ramponi, G., Nassi, P., & Treves, C. (1968) *Life Sci.* 7, 443−448.

Raugei, G., Modesti, A., Magherini, F., Marzocchini, R., Vecchi, M., & Ramponi, G. (1996) *Biotechnol. Appl. Biochem. 23*, 273−278.

Reinard, T., & Jacobsen, H. J. (1989) *Anal. Biochem. 176*, 157−160.

Sanger, F., Nicklen, S., & Coulson, A. R. (1977) *Proc. Natl. Acad. Sci. U.S.A.* 74, 5436.

Satchell, D. P. N., Spencer, N., & White, G. F. (1972) *Biochim. Biophys. Acta 268*, 233−248.

Saudek, V., Williams, R. J. P., Stefani, M., & Ramponi, G. (1989) *Eur. J. Biochem. 185*, 99−103.

Stefani, M., & Ramponi, G. (1995) *Life Chem. Rep. 12*, 271−301.

Stefani, M., Liguri, G., Berti, A., Nassi, P., & Ramponi, G. (1981) *Arch. Biochem. Biophys. 208*, 37−41.

Stites, W. E., Meeker, A. K., & Shortle, D. (1994) *J. Mol. Biol. 235*, 27−32.

Taddei, N., Stefani, M., Vecchi, M., Modesti, A., Raugei, G., Bucciantini, M., Magherini, F., & Ramponi, G. (1994a) *Biochim. Biophys. Acta 1208*, 75−80.

Taddei, N., Buck, M., Broadhurst, R. W., Stefani, M., Ramponi, G., & Dobson, C. M. (1994b) *Eur. J. Biochem. 225*, 811−817.

Taddei, N., Modesti, A., Bucciantini, M., Stefani, M., Magherini, F., Vecchi, M., Raugei, G., & Ramponi, G. (1995) *FEBS Lett. 362*, 175−179.

Taddei, N., Stefani, M., Magherini, F., Chiti, F., Modesti, A., Raugei, G., & Ramponi, G. (1996) *Biochemistry 35*, 7077−7083.

Thunnissen, M. M. G. M., Taddei, N., Liguri, G., Ramponi, G., & Nordlund, P. (1997) *Structure 5*, 69−79.

Toumadje, A., Alcorn, S. W., & Johnson, W. C. (1992) *Anal. Biochem. 200*, 321−331.

Wüthrich, K. (1986) in *NMR of Proteins and Nucleic Acids*, John Wiley & Sons, New York.

BI970173+